Heat Transfer Engineering, 27(5):23–38, 2006
Copyright © Taylor and Francis Group, LLC
ISSN: 0145-7632 print / 1521-0537 online
DOI: 10.1080/01457630600559538

Transitional Heat Transfer in Plain Horizontal Tubes

LAP MOU TAM
Department of Electromechanical Engineering, University of Macau, Taipa, Macau, China

AFSHIN J. GHAJAR
School of Mechanical and Aerospace Engineering, Oklahoma State University, Stillwater, Oklahoma, USA

In this study, the heat transfer behavior in the transition region for plain horizontal tubes under a uniform wall heat flux boundary condition is discussed in detail. In particular, the influence of inlet configuration and free convection superimposed on the forced convection (or mixed convection) at the start and end of the transition region and the magnitude of heat transfer are addressed. The available correlations to predict the heat transfer coefficient in the transition region are reviewed, and their performance are evaluated based on 1290 experimental data points obtained under a wide range of experimental conditions. Appropriate correlations for the mixed and forced convection transition regions are recommended. Finally, a flow regime map for determination of the boundary between forced and mixed convection in horizontal tubes with different inlets is presented.

INTRODUCTION

An important design problem in industrial heat exchangers arises when flow inside the tubes falls into the transition region. In practical engineering design, the usual recommendation is to avoid design and operation in this region; however, this is not always feasible under design constraints. The usually cited transitional Reynolds number range of about 2300 (the onset of turbulence) to 10,000 (fully turbulent condition) applies, strictly speaking, to a very steady and uniform entry flow with a rounded entrance. If the flow has the disturbed entrance typical of heat exchangers, in which there is a sudden contraction and possibly even a re-entrant entrance, the transitional Reynolds number range will be much different. This in turn influences the magnitude of heat transfer coefficient in this region.

The selection or development of an appropriate heat transfer correlation for the transition region in horizontal tubes requires an understanding of the factors that influence the start and end of the transition region and the behavior of heat transfer in this region.

The objective of this paper is to first gain an understanding of the factors influencing heat transfer in the transition region and then analyze the available heat transfer correlations for this region.

Address correspondence to Dr. Afshin J. Ghajar, School of Mechanical and Aerospace Engineering, Oklahoma State University, 218 Engineering North, Stillwater, OK 74078. E-mail: ghajar@ceat.okstate.edu

HEAT TRANSFER BEHAVIOR IN THE TRANSITION REGION

To gain a complete understanding of the heat transfer behavior in the transition region, the experimental results of Ghajar and his coworkers [1–3] will be examined. This is the most complete and systematic heat transfer experimental data set in the transition region available in the open literature. They experimentally investigated the inlet configuration effects on developing and fully developed transitional forced and mixed convection heat transfer in a circular tube under a uniform wall heat flux boundary condition. Their experiments were conducted in a circular tube with a maximum length-to-inside diameter ratio of 385. In their experiments, distilled water and mixtures of distilled water and ethylene glycol were used. They collected 1290 experimental data points, and their experiments covered a local bulk Reynolds number range of 280 to 49000, a local bulk Prandtl number range of 4 to 158, a local bulk Grashof number range of 1000 to 2.5×10^5, and a local bulk Nusselt number range of 13 to 258. The wall heat flux for their experiments ranged from 4 to 670 kW/m^2. In their investigations, they used three types of inlet configurations, as shown in Figure 1: re-entrant

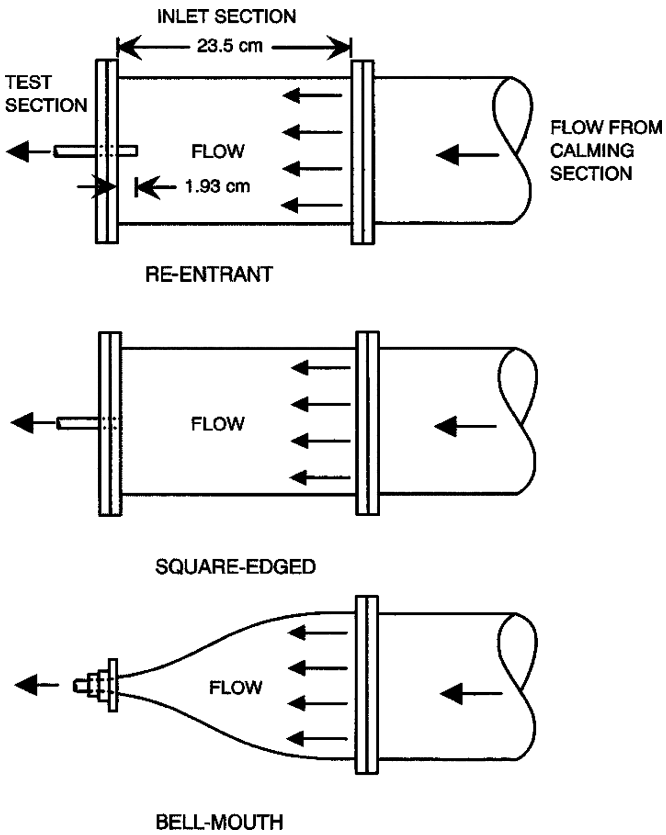

Figure 1 Schematic of the three different inlet configurations.

(tube extends beyond tubesheet face into the head of distributor), square-edged (tube end is flush with tubesheet face), and bell-mouth (a tapered entrance of tube from tubesheet face).

Figure 2 [1] clearly shows the influence of the inlet configuration on the beginning and end of the heat transfer transition region. This figure plots the local average peripheral heat transfer coefficients in terms of the Colburn j factor ($j = St\ Pr^{0.67}$) versus local Reynolds number for all flow regimes at the length-to-inside diameter ratio of 192. The filled symbols in Figure 2 designate the start and end of the heat transfer transition region for each inlet. The presented results show how heat transfer in the transition region varies between the limits of the Sieder and Tate [4]-type correlation [$Nu = 0.023Re^{0.8}Pr^{0.33}(\mu_b/\mu_w)^{0.14}$] for fully developed turbulent flow and $Nu = 4.364$ for fully developed laminar flow with a uniform wall heat flux boundary condition. Note the buoyancy effect on the laminar flow data giving the much larger mixed convection heat transfer coefficient, yielding a mixed convection value of about $Nu = 14.5$.

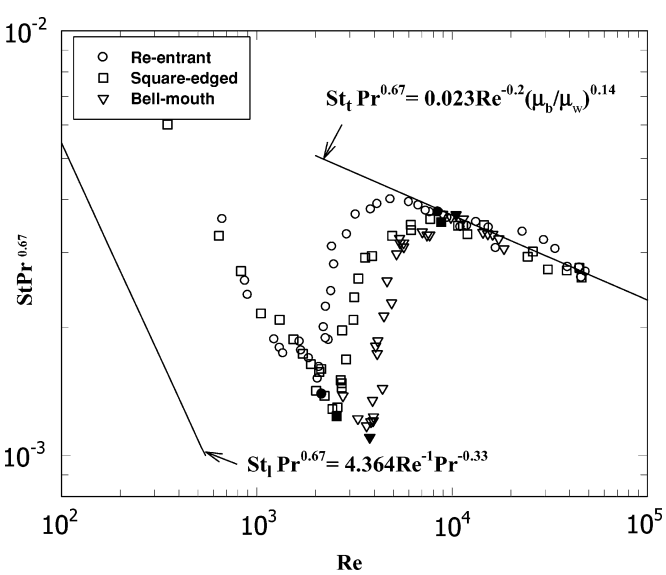

Figure 2 Heat transfer in the transition region (filled symbols designate the start and end of the transition region for each inlet).

As shown by the filled symbols in Figure 2, the lower and upper limits of the heat transfer transition Reynolds number range depend on the inlet configuration. In addition, these transition Reynolds number limits are x/D-dependent, and they linearly increase with an increase in x/D [2]. To determine the range of heat transfer transition Reynolds numbers along the tube, Ghajar and Tam [2] used their experimental data and developed figures similar to Figure 2 for twenty other x/D locations. From these figures, the heat transfer transition Reynolds number range for each inlet was determined to be about 2000–8500 for the re-entrant inlet, 2400–8800 for the square-edged inlet, and 3400–10,500 for the bell-mouth inlet. The lower and upper limits of the heat transfer transition Reynolds number ranges for the three different inlets along the tube ($3 \leq x/D \leq 192$) are summarized in Table 1. The results shown in this table indicate that the re-entrant inlet configuration causes the earliest transition from laminar flow into the transition regime (at about 2000), while the bell-mouth entrance retards this regime change (at about 3400). The square-edged entrance falls in between (at about 2400), which is close to the often quoted value of 2300 in most textbooks.

The application of heat to the tube wall produces a temperature difference in the fluid. The fluid near the tube wall has a higher temperature and lower density than the fluid close to the centerline of the tube. This temperature difference may produce a secondary flow due to free convection. In the laminar flow region, the effect of free convection (or buoyancy) on forced convection can be clearly seen in Figure 2, which resulted in an upward parallel shift of the Colburn j factors from their fully developed forced convection laminar values. In the transition region, the effect of mixed convection cannot be easily seen unless the local heat transfer information, which is the ratio of the local

Table 1 The lower and upper limits of the heat transfer transition Reynolds numbers

Inlet geometry	Lower limit	Upper limit
Re-entrant	$Re_{lower} = 2157 - 0.65\,[192 - (x/D)]$	$Re_{upper} = 8475 - 9.28\,[192 - (x/D)]$
Square-edged	$Re_{lower} = 2524 - 0.82\,[192 - (x/D)]$	$Re_{upper} = 8791 - 7.69\,[192 - (x/D)]$
Bell-mouth	$Re_{lower} = 3787 - 1.80\,[192 - (x/D)]$	$Re_{upper} = 10481 - 5.47\,[192 - (x/D)]$

peripheral heat transfer coefficient at the top of the tube to the local peripheral heat transfer coefficient at the bottom of the tube (h_t/h_b), is carefully examined. To properly account for the effect of mixed convection, Ghajar and his coworkers [1–3] used four thermocouples around the periphery of the tube (90° apart) at each of the twenty-six designated axial locations along the tube. The thermocouples were at close intervals near the entrance of the tube and at greater intervals further downstream. According to Ghajar and Tam [1, 2], h_t/h_b should be close to unity (0.8–1.0) for forced convection and is much less than unity (< 0.8) for a case in which mixed convection exists. Figure 3 [1, 2] shows the effect of secondary flow on heat transfer coefficient for different inlets and flow regimes. For the re-entrant, square-edged, and bell-mouth inlets, when the Reynolds numbers were greater than 2500, 3000, and 8000, respectively, the flows were dominated by forced convection heat transfer, and the heat transfer coefficient ratios (h_t/h_b) did not fall below 0.8–0.9. (In fact, at times they exceeded unity due to the roundoff errors in the property evaluation subroutine of their [1] data reduction program.) The flows dominated by mixed convection heat transfer had h_t/h_b ratios beginning near 1 but dropped off rapidly as the length-to-diameter ratio (x/D) increased. Beyond about 125 diameters from the entrance, the ratio was almost invariant with x/D, indicating a much less dominant role for forced convection heat transfer and increased free convection activity. In reference to Figure 3, it is interesting to observe that the starting length necessary for the establishment of the free convection effect for low Reynolds number flows is also inlet-dependent. When the secondary flow is established, a sharp decrease in h_t/h_b occurs. Depending on the type of inlet configuration, for low Reynolds number flows (Re < 2500 for re-entrant, < 3000 for square-edged, and < 8000 for bell-mouth), the flow can be considered to be dominated by forced convection over the first 20–70 diameters from the entrance to the tube. It should be noted that the reported lower and upper limits of heat transfer transition Reynolds numbers in Table 1 are not influenced by the presence of mixed convection. However, as the flow travels the tube length required for the establishment of secondary flow, the lower transition region for all three inlets will be influenced by the presence of mixed convection. It should be noted that for the bell-mouth inlet, the mixed convection effect will influence not only the lower transition region but also the upper part of the transition region [3].

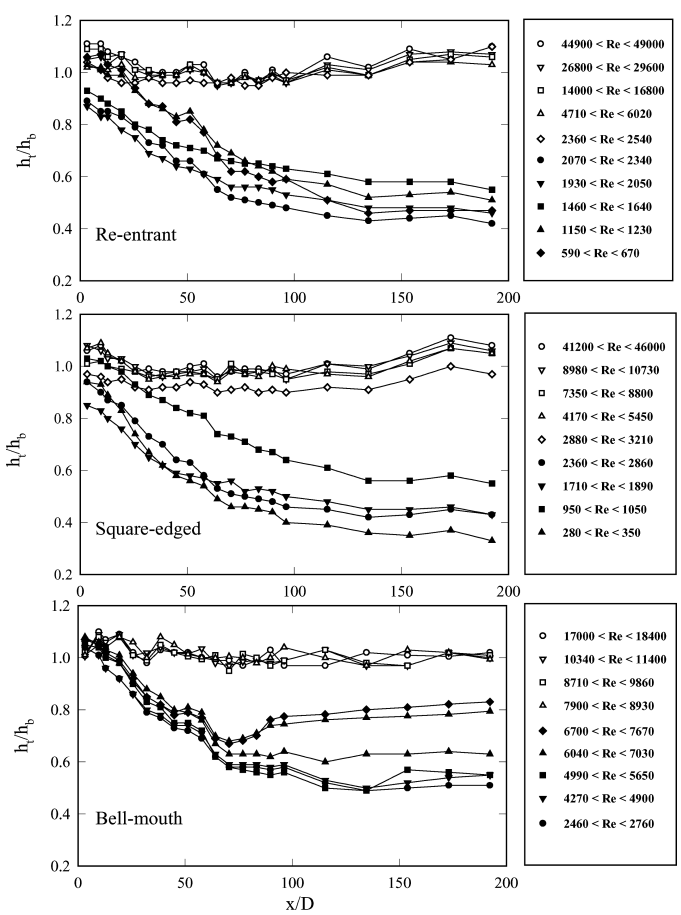

Figure 3 Effect of secondary flow on heat transfer coefficient for different inlets and flow regimes.

In a subsequent study, Tam and Ghajar [3] experimentally investigated the behavior of local heat transfer coefficients in the transition region for a tube with a bell-mouth inlet. This type of inlet is used in some heat exchangers mainly to avoid the presence of eddies that are believed to be one of the causes for erosion in the tube inlet region. Figure 4 shows the variation of local Nusselt number along the tube length (x/D) in the transition region for the three inlet configurations at comparable Reynolds numbers. As shown in Figure 4, the re-entrant and square-edged inlets show no influence on the local heat transfer coefficients. For these inlets, the local Nusselt number has a minimum value at an x/D approximately equal to 25 and increases monotonically along the tube rather than staying at a relatively constant value, as is the expected behavior in the fully developed laminar and turbulent flows (see Figure 5) [3]. However, for the bell-mouth inlet, the variation of the local heat transfer coefficient with tube length in the transition (Figure 4) and turbulent (Figure 5) flow regions is very unusual. For this inlet geometry, the boundary layer along the tube wall is at first laminar and then changes through a transition to the turbulent condition, causing a dip in the Nu vs. x/D curve. The length of the dip in the transition region is much longer ($100 < x/D < 175$) than in the turbulent region ($x/D < 25$), as shown in Figures 4 and 5, respectively. Hence, the mixed convection effect is strongly present even in high Reynolds numbers' upper transition region. The presence of the dip in the transition region causes a significant influence in both the local and average heat transfer coefficients. This is particularly important for heat transfer calculations in short tube heat exchangers with a bell-mouth inlet.

HEAT TRANSFER CORRELATIONS IN THE TRANSITION REGION

The first correlation that received attention is the one proposed by Hausen [5], as the proposed correlation covers

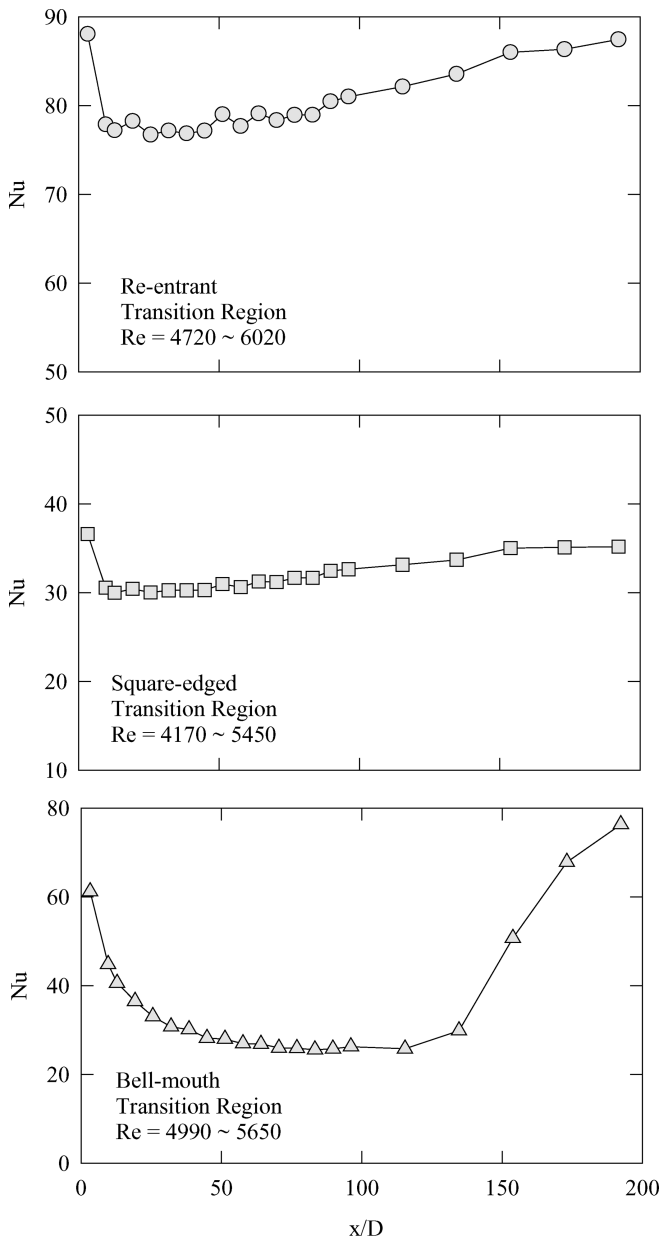

Figure 4 Variation of local Nusselt number with length for the re-entrant, square-edged, and bell-mouth inlets in the transition region.

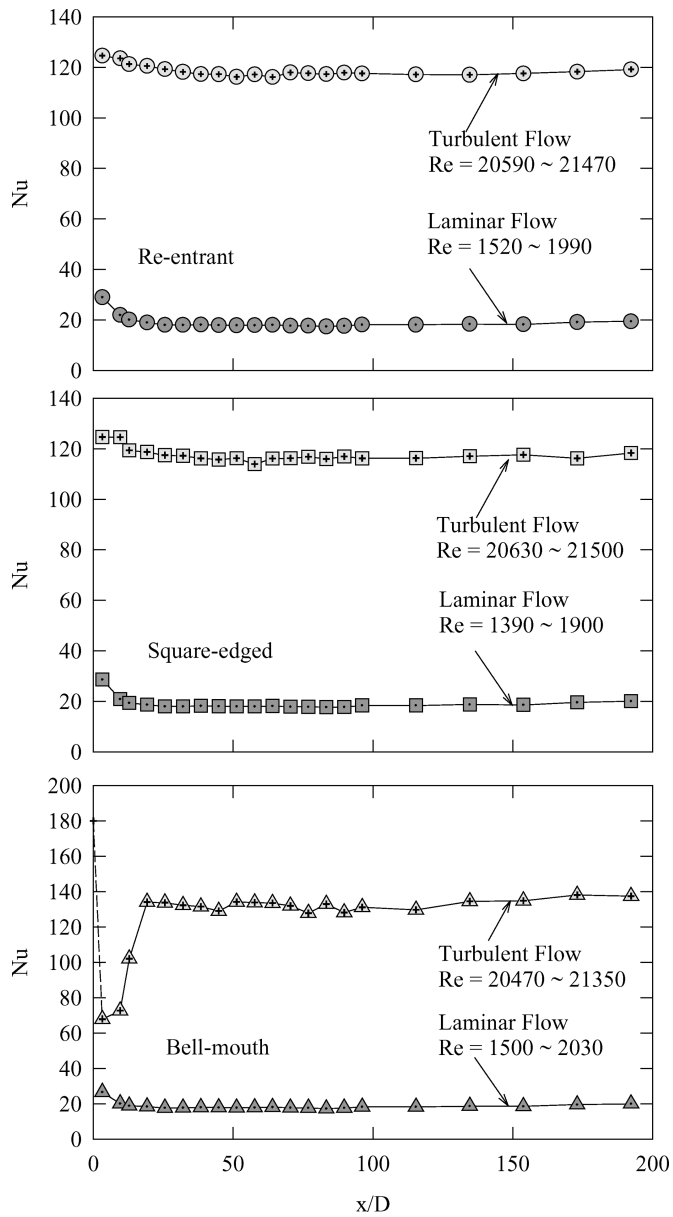

Figure 5 Variation of local Nusselt number with length for the re-entrant, square-edged, and bell-mouth inlets in the laminar and turbulent regions.

Reynolds numbers ranging from 2300 to 10^5. This correlation was developed using the data collected in [4]. The form of this correlation, which is the product of different exponential functions, is in a form typical of turbulent flow correlations. Hausen's correlation is:

$$\mathrm{Nu} = 0.037(\mathrm{Re}^{0.75} - 180)\mathrm{Pr}^{0.42}\left[1 + \left(\frac{\mathrm{D}}{\mathrm{x}}\right)^{2/3}\right]\left(\frac{\mu_b}{\mu_w}\right)^{0.14} \quad (1)$$

where $0 < \mathrm{D/x} < 1$ and $0.6 < \mathrm{Pr} < 10^3$.

Equation (1) was examined by various researchers after its publication in 1959. Researchers such as Hufschmidt et al. [6], Reinicke [7], and Schlunder [8] indicated that their experimental heat transfer coefficients deviated considerably from the values predicted by Hausen's correlation in the transition region, and therefore should limit the applicability of this equation in the transition region. Even though Hausen's correlation proved to be not accurate in the transition region, there is little follow-up research in this important region.

According to the *Handbook of Single-Phase Convective Heat Transfer* [9], the correlations that can be used in the fully developed transition region are those of Gnielinski [10] and Churchill [11], based on the listed Reynolds number range. The correlations by Gnielinski [10] are also strongly recommended by Shah and Johnson [12]. Gnielinski's correlation is based on the correlation form of Petukhov et al. [13], which is in fact an improved version of Prandtl's [14] correlation. Gnielinski's correlation is

given as:

$$\mathrm{Nu} = \frac{\left(\frac{f}{2}\right)(\mathrm{Re} - 1000)\,\mathrm{Pr}}{1 + 12.7\left(\frac{f}{2}\right)^{0.5}(\mathrm{Pr}^{2/3} - 1)} \tag{2}$$

where $2300 < \mathrm{Re} < 5 \times 10^6$, $0.5 < \mathrm{Pr} < 2000$, and $f = (1.58\ln\mathrm{Re} - 3.28)^{-2}$.

For the developing region, Gnielinski modified Eq. (2) by introducing the correction factors $[1 + (D/x)^{2/3}]$, which takes care of the entrance effects, and $(\mathrm{Pr_b}/\mathrm{Pr_w})^{0.11}$, which considers the influence of emperature-dependent fluid properties. The Prandtl number ratio can be approximated by $(\mu_b/\mu_w)^{0.11}$ because $\mathrm{Pr} = \mu c_p/k$, and for most liquids, the thermal conductivity and specific heat are relatively independent of temperature. Therefore, for developing liquid flow, Gnielinski's correlation took the following form:

$$\mathrm{Nu} = \frac{\left(\frac{f}{2}\right)(\mathrm{Re} - 1000)\,\mathrm{Pr}}{1 + 12.7\left(\frac{f}{2}\right)^{0.5}(\mathrm{Pr}^{2/3} - 1)}\left[1 + \left(\frac{D}{x}\right)^{2/3}\right]\left(\frac{\mu_b}{\mu_w}\right)^{0.11} \tag{3}$$

where

$$f = (1.58\ \ln\mathrm{Re} - 3.28)^{-2}.$$

This correlation is good for developing forced convection with a Reynolds number ranging from 2300 to 10^6 and a Prandtl number ranging from 0.6 to 10^5. In establishing the constants in his correlation, Gnielinski made use of approximately 800 experimental data points from various researchers. Details regarding the data used by Gnielinski are available in [10]. According to Gnielinski, nearly 90% of the experimental data were predicted with less than ±20% deviation.

Another important correlation for the transition region is the correlation of Churchill [11]. The general expression of the correlation is of the form:

$$\mathrm{Nu}^{10} = \mathrm{Nu}_l^{10} + \left[\frac{\exp[(2200 - \mathrm{Re}/365)]}{\mathrm{Nu}_{lc}^2} + \frac{1}{\mathrm{Nu}_t^2}\right]^{-5} \tag{4}$$

where Nu_l is the correlation for the laminar Nusselt number, Nu_{lc} is the Nusselt number being evaluated at critical Reynolds number of 2100, and Nu_t is correlation for the turbulent Nusselt

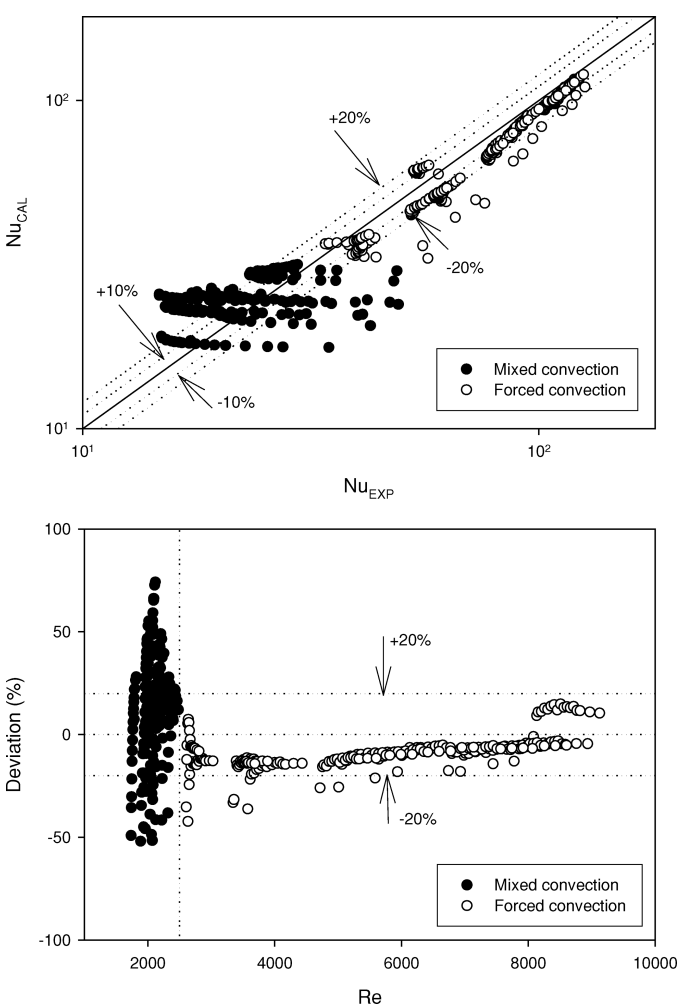

Figure 6 Comparison between predictions of Eq. (2) and experimental data for the re-entrant inlet.

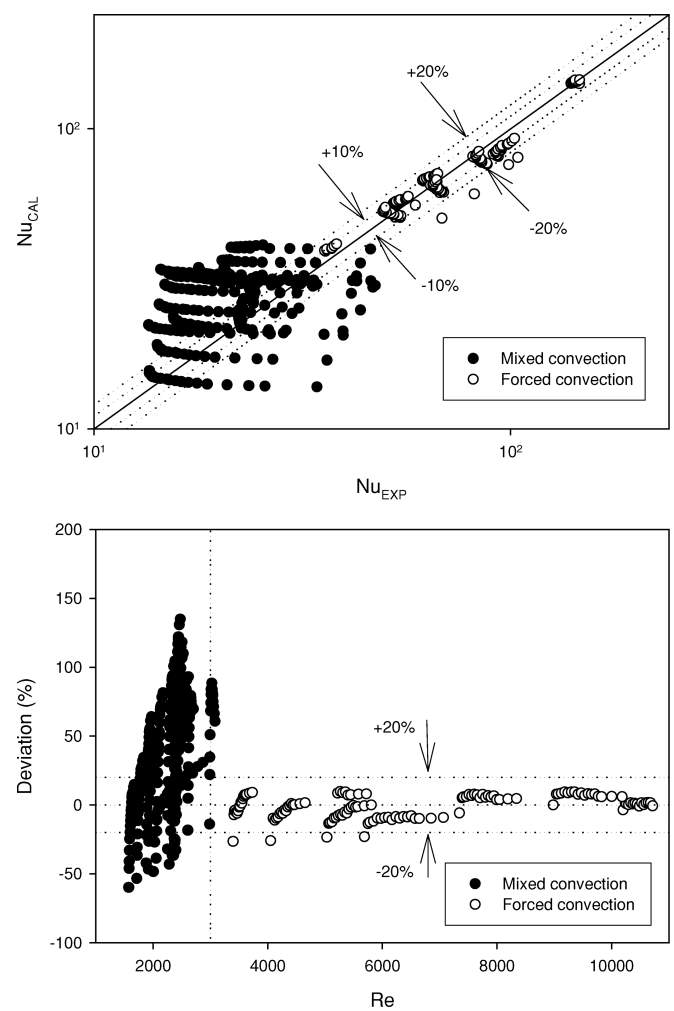

Figure 7 Comparison between predictions of Eq. (2) and experimental data for the square-edged inlet.

number. With the appropriate values for Nu_l, Nu_{lc}, and Nu_t, Churchill's equation is capable of predicting hydrodynamically and thermally fully developed flow and hydrodynamically fully developed and thermally developing flow. For hydrodynamically and thermally fully developed flow, the equations for Nu_l, Nu_{lc}, and Nu_t are:

$$Nu_l = Nu_{lc} = 4.36$$

and

$$Nu_t = 6.3 + \frac{0.079(f/2)^{1/2} Re\, Pr}{(1 + Pr^{4/5})^{5/6}}$$

where

$$\frac{1}{\sqrt{f}} = 2.21 \ln\left(\frac{Re}{7}\right)$$

Therefore, Churchill's correlation for hydrodynamically and thermally fully developed flow becomes:

$$Nu^{10} = (4.364)^{10} + \left[\frac{\exp[(2200 - Re/365)]}{(4.364)^2} + \frac{1}{Nu_t^2}\right]^{-5} \quad (5)$$

For hydrodynamically fully developed and thermally developing flow, the values of Nu_l and Nu_{lc} are no longer constant, and the following equations should be used instead:

$$Nu_l = 4.364\left[1 + \left(\frac{Re\, Pr\, D/x}{7.3}\right)^2\right]^{1/6}$$

$$Nu_{lc} = 4.364\left[1 + \left(\frac{287\, Pr\, D}{x}\right)^2\right]^{1/6}$$

For moderate to large Prandtl numbers, the thermal entrance effect is negligible according to [11]; therefore, the same Nu_t equation recommended for use in Eq. (5) can still be used. Hence, Churchill's correlation for hydrodynamically developing and thermally fully developed flow becomes:

$$Nu^{10} = \left\{4.364\left[1 + \left(\frac{Re\, Pr\, D/x}{7.3}\right)^2\right]^{\frac{1}{6}}\right\}^{10} + \left[\frac{\exp[(2200 - Re/365)]}{Nu_{lc}^2} + \frac{1}{Nu_t^2}\right]^{-5} \quad (6)$$

In the development of his correlation, Churchill [11] took a completely different approach than the one taken by Gnielinski.

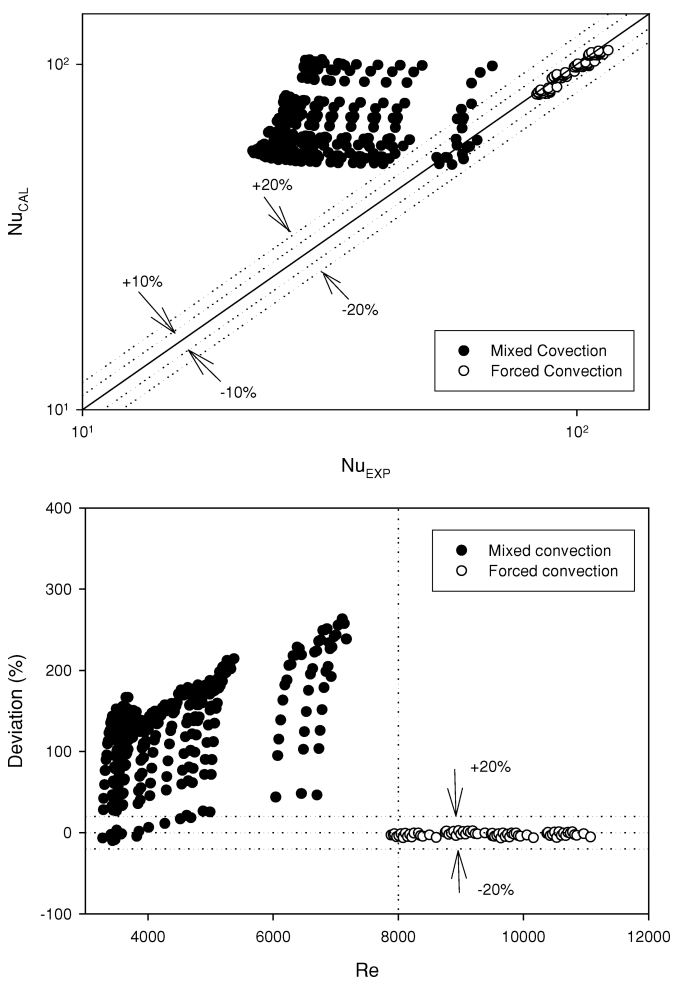

Figure 8 Comparison between predictions of Eq. (2) and experimental data for the bell-mouth inlet.

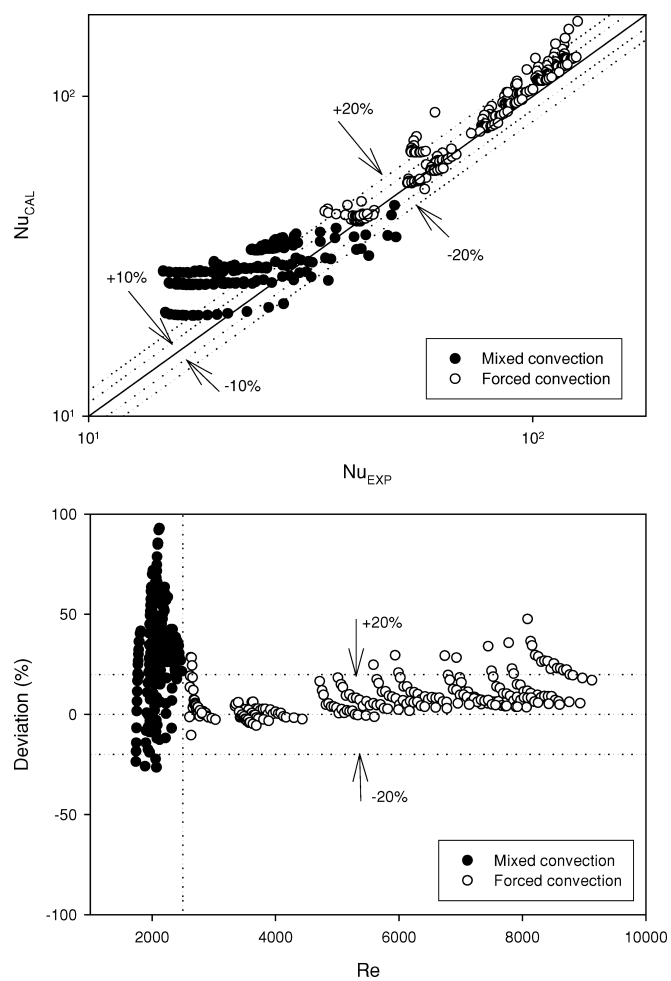

Figure 9 Comparison between predictions of Eq. (3) and experimental data for the re-entrant inlet.

In Gnieslinski's work, even though it was not mentioned explicitly by the author but is apparent from the experimental data used in his work, the majority of the data were in the fully turbulent region (Reynolds numbers greater than 8000). Therefore, Gnielinski considered his correlation suitable for turbulent pipe and channel flows. However, Churchill's correlation was developed for the entire flow regime (laminar, transition, and turbulent) with Reynolds numbers ranging from 10 to 10^6 and Prandtl numbers ranging from 0 to 10^6. The method used by Churchill was first proposed in the work of Churchill and Usagi [15]. They successfully implemented a heat transfer correlation that can be constructed by taking the pth root of the sum of the pth power of the limiting solutions or correlations for large and small values of the independent variable. Intermediate values were then utilized to choose the best value for the arbitrary exponent p.

This procedure was first used to construct an expression for the effect of Pr on Nu at large Re values. This correlating equation for large Re values was then combined with a value of Nu for the limiting case of turbulent flow as RePr decreases to yield a correlating equation for all Pr values over the entire regime of fully developed turbulent flow. This second correlating equation was in turn combined with an asymptotic expression for transition to laminar flow. Finally, this third correlating equation was combined with the appropriate expression for Nu in the laminar regime to give an overall correlating equation for all Re and Pr values. With the use of appropriate sub-correlations, Churchill's correlation seems to work for both developing and fully developed flows.

Churchill [11] collected experimental data from other researchers to examine his correlation. He used a total number of 249 experimental data points in the Prandtl number range of 0.022 to 75 and Reynolds number range of 10^3 to 10^6. Churchill claimed that the accuracy of his correlation is comparable to Gnielinski's correlation (i.e., nearly 90% of the experimental data were predicted with less than 20% deviation), but the application range is broader because of the method used in setting up the correlation. Churchill [11] clearly recognized the importance of accurate experimental data, particularly in the transition region, and clearly states that the modification of the coefficients and exponents of his correlation is necessary when measurements with improved accuracy can be obtained in the future.

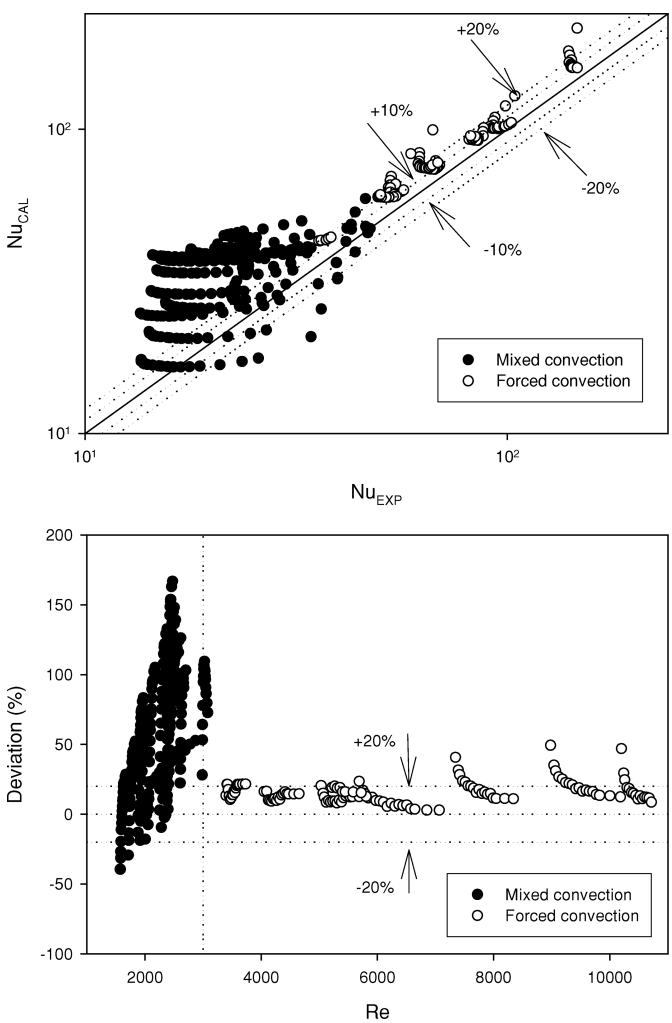

Figure 10 Comparison between predictions of Eq. (3) and experimental data for the square-edge inlet.

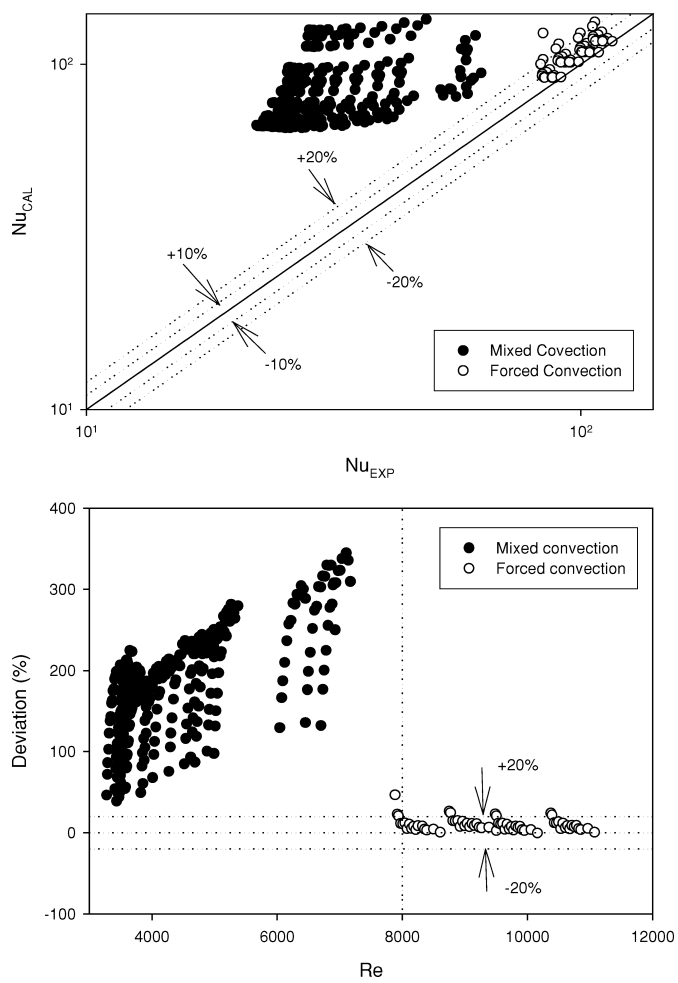

Figure 11 Comparison between predictions of Eq. (3) and experimental data for the bell-mouth inlet.

Neither of the correlations presented so far were specifically developed for the transition region. In Gnielinski's work attention was given mostly to the turbulent region; in Chruchill's work, the main contribution was to develop a single correlation for all flow regimes instead of a precise correlation just for the transition region. In developing their transition region heat transfer correlations, Ghajar and Tam [1] took a completely different approach than the previous investigators in this region. They first performed very careful experiments in the transition region, paying particular attention to the role of secondary flow (free convection superimposed on the forced convection or mixed convection) and inlet configuration effects on the start and end of the transition region and the magnitude of heat transfer in this region. After a careful analysis of their transitional heat transfer and following the general form of Churchill's [11] correlation, Ghajar and Tam [1] proposed some prediction methods for this region to bridge between laminar correlations and turbulent correlations and applicable to forced and mixed convection in the entrance and fully developed regions for three types of inlet configurations (re-entrant, square-edged, and bell-mouth). The local heat transfer coefficient in transition flow is obtained from the transition Nusselt number, Nu_{trans}, which is calculated as follows at a distance x from the entrance:

$$Nu_{trans} = Nu_l + \{\exp[(a - Re)/b] + Nu_t^c\}^c \tag{7}$$

where Nu_l is the laminar flow Nusselt number and Nu_t is the turbulent flow Nusselt number given by Eqs. (8) and (9), respectively.

Ghajar and Tam [1] used a total of 546 experimental data points in the entrance and fully developed laminar region with natural convection effects and proposed the following correlation for the laminar flow Nusselt number (Nu_l), which represented 86% of experimental data with less than ±10% deviation and 100% of measured data with less than ±17% deviation:

$$Nu_l = 1.24\left[\left(\frac{Re\,Pr\,D}{x}\right) + 0.025(Gr\,Pr)^{0.75}\right]^{1/3}\left(\frac{\mu_b}{\mu_w}\right)^{0.14} \tag{8}$$

where $3 \le x/D \le 192$, $280 \le Re \le 3800$, $40 \le Pr \le 160$, $1000 \le Gr \le 28000$, and $1.2 \le \mu_b/\mu_w \le 3.8$. For a turbulent flow Nusselt number (Nu_t), Ghajar and Tam [1] used a total of 604 experimental data points in the entrance and fully developed

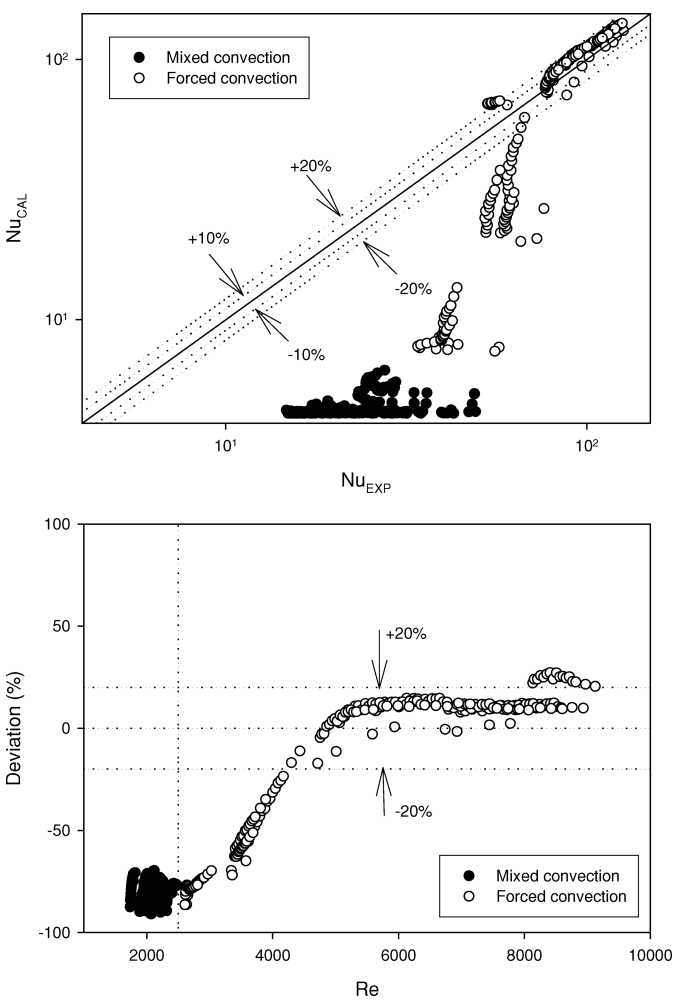

Figure 12 Comparison between predictions of Eq. (5) and experimental data for the re-entrant inlet.

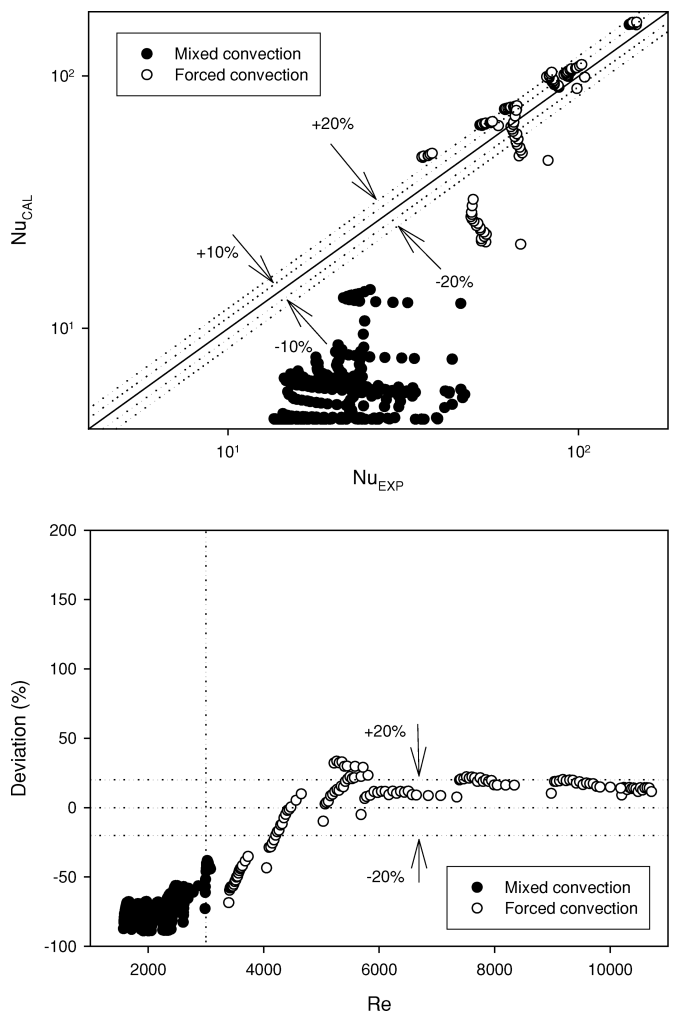

Figure 13 Comparison between predictions of Eq. (5) and experimental data for the square-edged inlet.

turbulent region and developed the following correlation, correlating 100% of experimental data with less than ±11% deviation and 73% of measured data with less than ±5% deviation:

$$\mathrm{Nu_t} = 0.023\mathrm{Re}^{0.8}\mathrm{Pr}^{0.385}\left(\frac{x}{D}\right)^{-0.0054}\left(\frac{\mu_b}{\mu_w}\right)^{0.14} \tag{9}$$

where

$3 \le x/D \le 192$,
$7000 \le \mathrm{Re} \le 49000$,
$4 \le \mathrm{Pr} \le 34$,
$1.1 \le \mu_b/\mu_w \le 1.7$.

The physical properties (k, μ, ρ, c_p) appearing in the dimensionless numbers (Nu, Re, Pr, Gr) are all evaluated at the bulk fluid temperature (T_b). The values of the empirical constants a, b, and c in Eq. (7) depend on the inlet configuration and are given in Table 2. The viscosity ratio accounts for the temperature effect on the process. The range of application of the heat transfer correlation based on Ghajar and Tam's [1] database of 1290 data points (441 points for re-entrant inlet, 416 points for square-edged inlet and 433 points for bell-mouth inlet) is as follows:

Table 2 Constants for transition heat transfer correlation

Inlet geometry	a	b	c
Re-entrant	1766	276	−0.955
Square-edged	2617	207	−0.950
Bell-mouth	6628	237	−0.980

Re-entrant. $3 \le x/D \le 192$, $1700 \le \mathrm{Re} \le 9100$, $5 \le \mathrm{Pr} \le 51$, $4000 \le \mathrm{Gr} \le 210000$, $1.2 \le \mu_b/\mu_w \le 2.2$.
Square-edged. $3 \le x/D \le 192$, $1600 \le \mathrm{Re} \le 10700$, $5 \le \mathrm{Pr} \le 55$, $4000 \le \mathrm{Gr} \le 250000$, $1.2 \le \mu_b/\mu_w \le 2.6$.
Bell-mouth. $3 \le x/D \le 192$, $3300 \le \mathrm{Re} \le 11100$, $13 \le \mathrm{Pr} \le 77$, $6000 \le \mathrm{Gr} \le 110000$, $1.2 \le \mu_b/\mu_w \le 3.1$.

These correlations capture about 70% of measured data within a deviation band of ±10% and 97% of measured data within ±20%, which is remarkable for transition flows. The individual expressions above for $\mathrm{Nu_l}$ and $\mathrm{Nu_t}$ can be used alone for developing and fully developed flows in those respective regimes. The lower and upper limits of the heat transfer transition Reynolds number ranges for the three different inlets are summarized in Table 1.

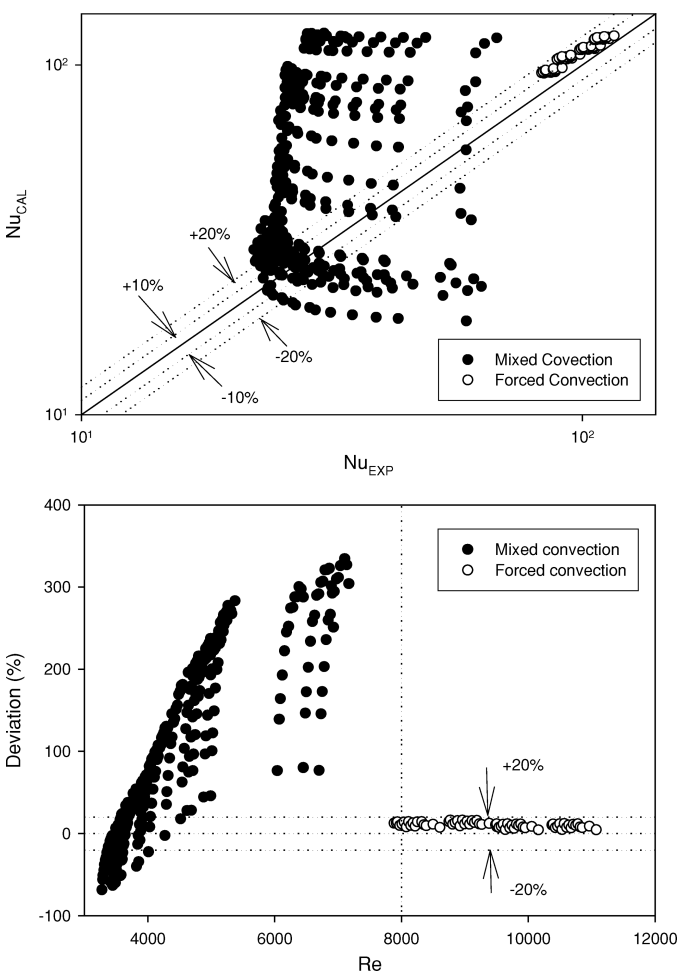

Figure 14 Comparison between predictions of Eq. (5) and experimental data for the bell-mouth inlet.

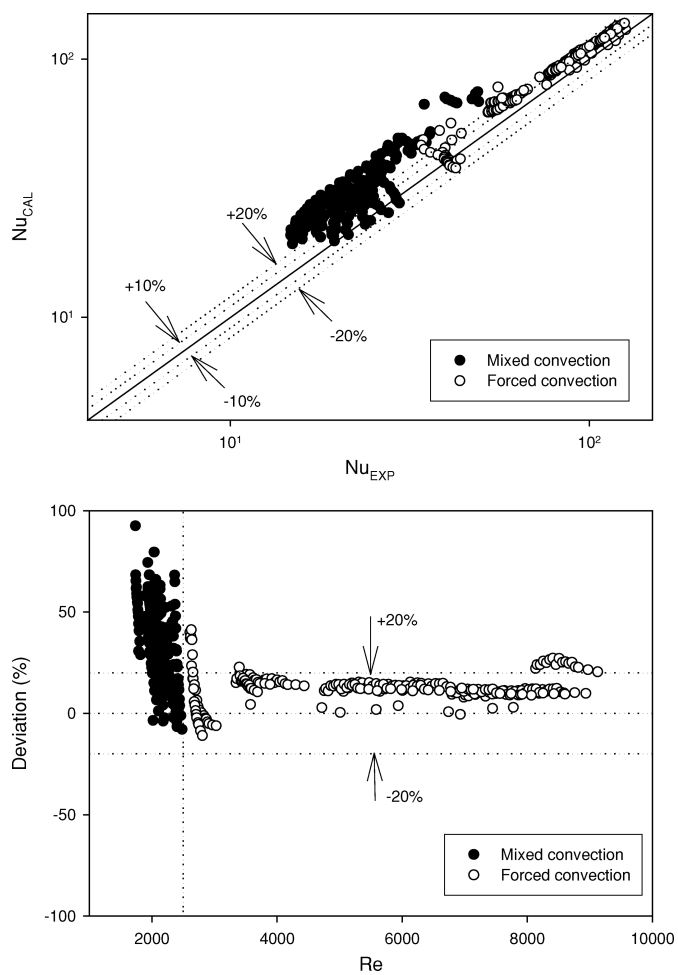

Figure 15 Comparison between predictions of Eq. (6) and experimental data for the re-entrant inlet.

COMPARISON OF THE ACCURACY OF THE CORRELATIONS

In this section, it will be shown how well the correlations of Gnielinski [10], Eqs. (2) and (3); Churchill [11], Eqs. (5) and (6); and Ghajar and Tam [1], Eq. (7) predict the developing and fully developed transitional flow experimental data of Ghajar and Tam [1] for the three different inlet configurations. The data for each inlet configuration were separated into two groups: the developing and fully developed mixed convection data, and the developing and fully developed forced convection data. The 441 data points for the re-entrant inlet consisted of 194 mixed convection and 247 forced convection data points. For the square-edged inlet with a total of 416 data points, 286 points were mixed convection and 130 data points were forced convection. For the third inlet, the bell-mouth, from a total of 433 data points, there were 365 mixed convection and 68 forced convection data points.

Figures 6 to 20 compare the predicted and experimental Nusselt numbers. In these figures, the boundary between the forced and mixed convection is also included to show the influence of mixed convection on the heat transfer in the transition region. As discussed earlier, the boundary for each inlet was determined by observing the ratio of the local peripheral heat transfer coefficient at the top of the tube to the local peripheral heat transfer coefficient at the bottom of the tube (h_t/h_b). The deviation between the predicted and the experimental Nusselt numbers for the five correlations under study is summarized in Tables 3 to 8 for the two groups of transitional experimental data (developing/fully developed mixed convection and developing/fully developed forced convection) and the three inlets (re-entrant, square-edged, and bell-mouth). For each case, the tables provide information on the number of the predicted data points that were within the ±5%, ±10–20%, ±20–30%, and above ±30% of the experimental data points. In addition, the absolute maximum, minimum, and average deviations for each correlation are presented. The last row of the tables shows what is referred to as a "±20% Index." This index shows the percentage of the total number of experimental data points that were predicted by a particular equation within ±20% deviation. This index will be used as a guideline to compare the performance of the different correlations under study. Figures 6 to 20 and Tables 3 to 8 clearly show the performance of these correlations in the transition region.

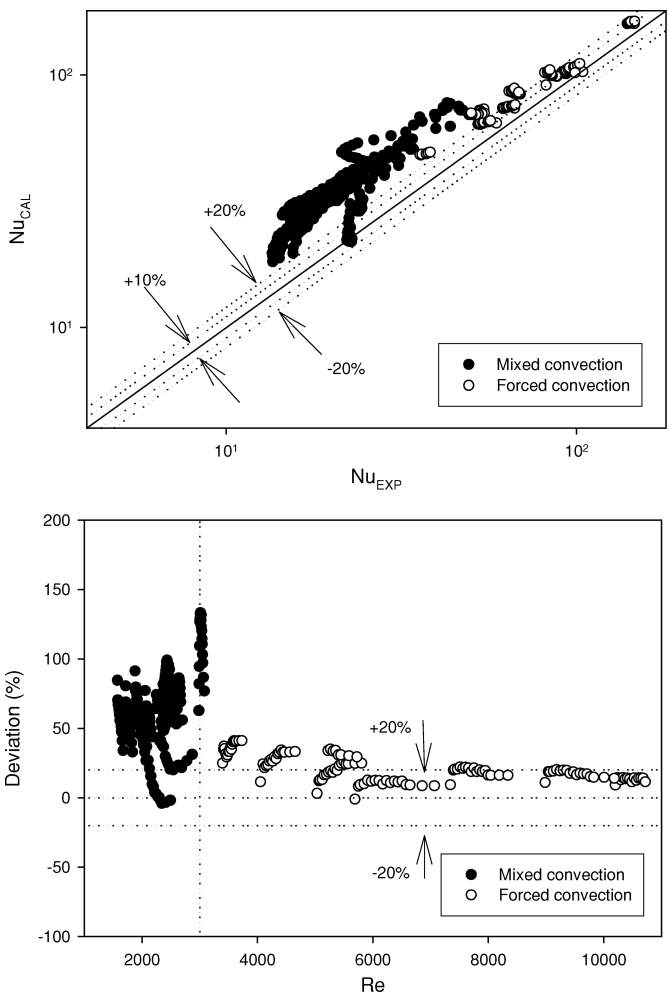

Figure 16 Comparison between predictions of Eq. (6) and experimental data for the square-edged inlet.

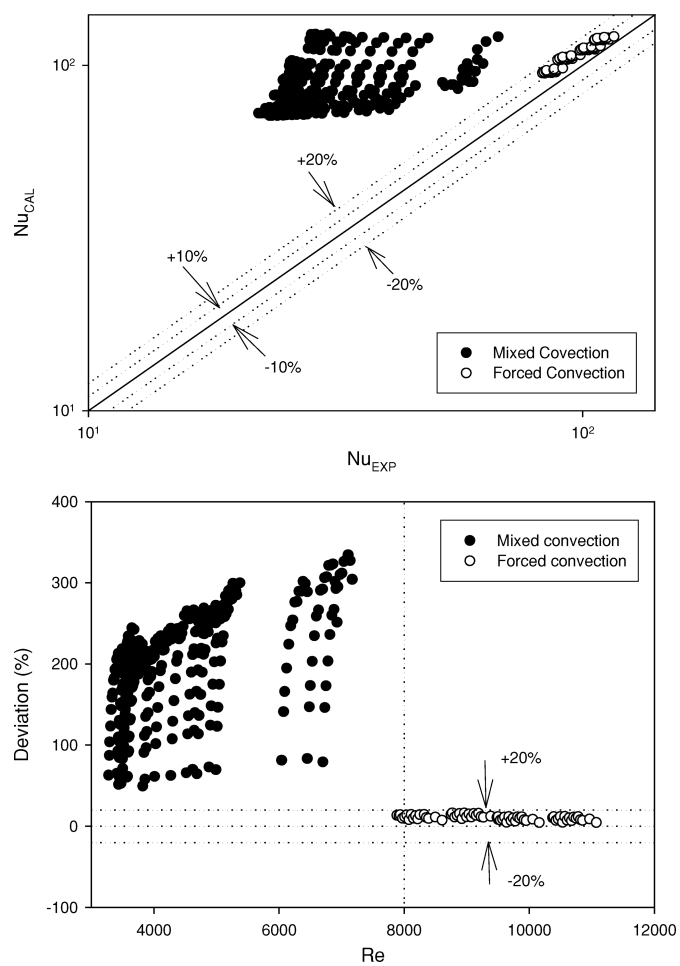

Figure 17 Comparison between predictions of Eq. (6) and experimental data for the bell-mouth inlet.

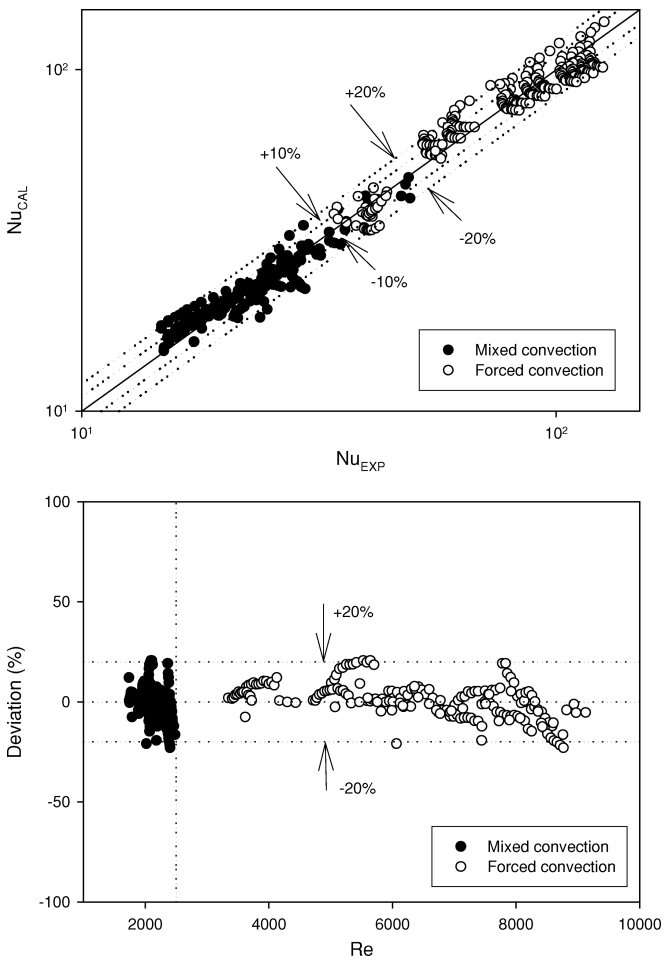

Figure 18 Comparison between predictions of Eq. (7) and experimental data for the re-entrant inlet.

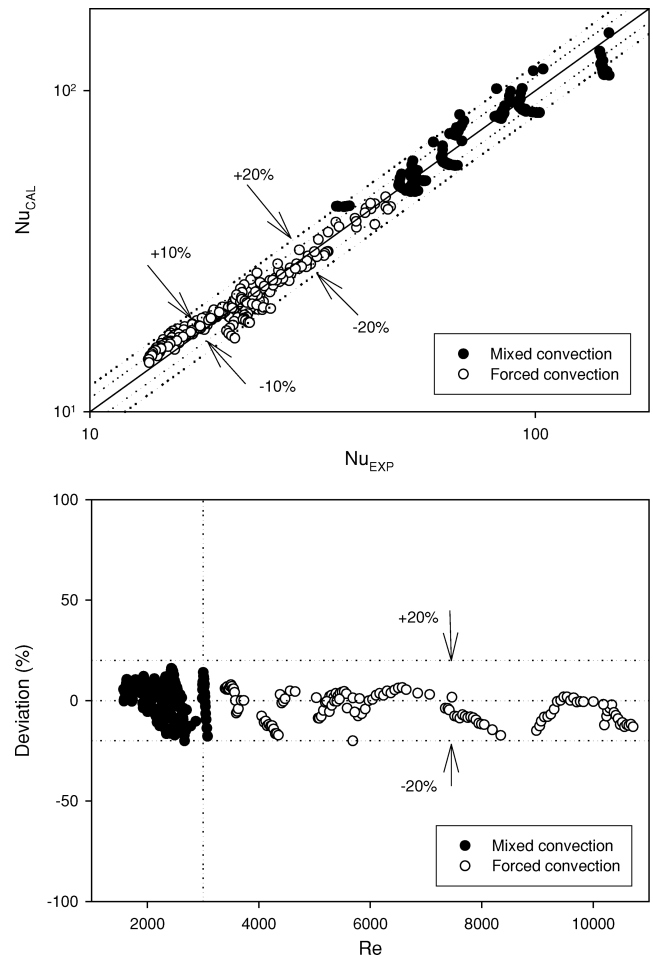

Figure 19 Comparison between predictions of Eq. (7) and experimental data for the square-edged inlet.

Gnielinski's correlations, Eqs. (2) and (3), are unable to provide satisfactory predictions of the experimental data in the mixed convection region for the three inlet configurations (see Figures 6 to 8 for Eq. [2] and Figures 9 to 11 for Eq. [3] for the results of comparisons). According to Tables 3, 5, and 7, Eq. (2) predicted only 48.5% of the data for the re-entrant inlet, 28.7% of the data for the square-edged inlet, and 4.1% of the data for the bell-mouth inlet with less than 20% deviation. For Eq. (3), the predictions were worse. The percentage of the data predicted with less than 20% deviation is 24.7% for the re-entrant inlet, 15.4% for the square-edge inlet, and none of the data of the bell-mouth inlet. However, for forced convection, it is a completely different situation. As shown in Figures 6 to 11, Eqs. (2) and (3) predicted the experimental data for all three inlets very accurately. According to Tables 4, 6 and 8, Eq. (2) predicted 96% of the data for the re-entrant inlet, 96.9% of the data for the square-edged inlet, and 100% of the data for the bell-mouth inlet with less than 20% deviation. Using Eq. (3), 89.1% of the data for the re-entrant inlet, 77.7% of the data for the square-edged inlet, and 86.8% of the data for the bell-mouth inlet were predicted with less than 20% deviation. Overall, the deviation band for Eqs. (2) and (3) is small, and the majority of the data were predicted with acceptable deviation.

Churchill's correlations, Eqs. (5) and (6), also failed to give an accurate prediction of the experimental data in the mixed convection region for the three inlet configurations, as depicted in Figures 12 to 14 for Eq. (5) and Figures 15 to 17 for Eq. (6). According to Tables 3, 5, and 7, the majority of the data were predicted with a deviation larger than 30% by both equations. However, the performance of Eqs. (5) and (6) were slightly better when they were applied to the bell-mouth inlet. For forced convection, according to Tables 4, 6, and 8, Eq. (5) predicted 59.5%, 64.6%, and 100% of the data with less than 20% deviation for the re-entrant, square-edged, and bell-mouth inlets, respectively. These results are also shown in Figures 12 to 14. Using Eq. (6), it predicted 89.5%, 54.6%, and 100% of the data with less than 20% deviation for the re-entrant, square-edged, and bell-mouth inlets, respectively (see also Figures 15 to 17 for the results of comparisons). From these comparisons, it is apparent that Eqs. (5) and (6) do an excellent job of predicting the forced convection data for the bell-mouth inlet. Equation (6) also does a very good job of predicting the forced convection data for the re-entrant inlet.

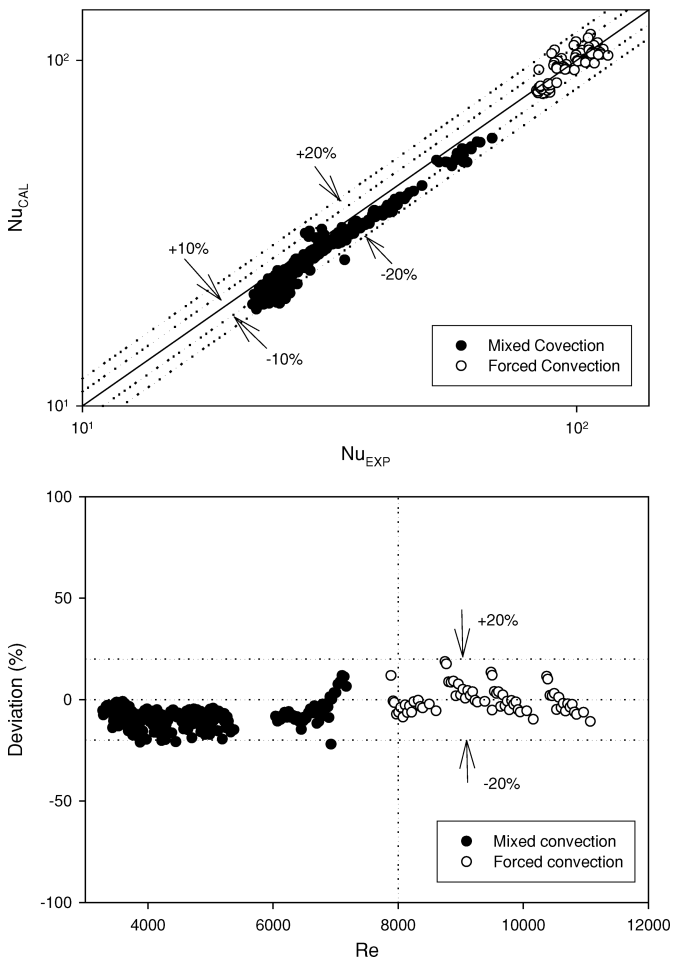

Figure 20 Comparison between predictions of Eq. (7) and experimental data for the bell-mouth inlet.

Ghajar and Tam's correlation, Eq. (7), predicted 96.9%, 99.7%, and 98.9% of the data in the mixed convection region with less than 20% deviation for the re-entrant, square-edged, and bell-mouth inlets, respectively. The results of these comparisons can be seen in Tables 3, 5, and 7, and Figures 18 to 20. In the forced convection region, according to Tables 4, 6, and 8, Eq. (7) predicted 97.2% (re-entrant inlet), 90.8% (square-edged inlet), and 100% (bell-mouth inlet) of the experimental data with less

Table 3 Deviations associated with different correlations (mixed convection re-entrant inlet, 194 data points)

Deviation range	Eq. (2)	Eq. (3)	Eq. (5)	Eq. (6)	Eq. (7)
Number of points below ±5%	18.00	8.00	0.00	13.00	89.00
Number of points between ±5–10%	21.00	15.00	0.00	8.00	68.00
Number of points between ±10–20%	55.00	25.00	0.00	22.00	31.00
Number of points between ±20–30%	46.00	34.00	0.00	20.0	6.00
Number of points above ±30%	54.00	112.00	194.00	131.00	0.00
Absolute maximum deviation %	74.15	92.98	91.01	92.49	23.00
Absolute minimum deviation %	0.57	0.22	69.58	0.36	0.02
Absolute average deviation %	23.64	33.70	78.67	37.61	6.61
±20% index	48.45	24.74	0.00	22.16	96.91

Table 4 Deviations associated with different correlations (forced convection re-entrant inlet, 247 data points)

Deviation range	Eq. (2)	Eq. (3)	Eq. (5)	Eq. (6)	Eq. (7)
Number of points below ±5%	18.00	102.00	16.00	23.00	68.00
Number of points between ±5–10%	104.00	75.00	38.00	30.00	75.00
Number of points between ±10–20%	115.00	43.00	93.00	168.00	97.00
Number of points between ±20–30%	5.00	22.00	21.00	21.00	7.00
Number of points above ±30%	5.00	5.00	79.00	5.00	0.00
Absolute maximum deviation %	42.27	47.64	86.45	41.22	25.12
Absolute minimum deviation %	1.04	0.03	0.54	0.24	0.09
Absolute average deviation %	10.65	8.67	28.35	13.12	9.02
±20% index	95.95	89.07	59.51	89.47	97.17

Table 5 Deviations associated with different correlations (mixed convection square-edged inlet, 286 data points)

Deviation range	Eq. (2)	Eq. (3)	Eq. (5)	Eq. (6)	Eq. (7)
Number of points below ±5%	24.00	11.00	0.00	8.00	121.00
Number of points between ±5–10%	16.00	10.00	0.00	2.00	104.00
Number of points between ±10–20%	42.00	23.00	0.00	2.00	60.00
Number of points between ±20–30%	31.00	31.00	0.00	14.00	1.00
Number of points above ±30%	173.00	211.00	286.00	260.00	0.00
Absolute maximum deviation %	134.91	166.84	88.98	133.32	20.02
Absolute minimum deviation %	0.20	0.37	38.13	0.39	0.01
Absolute average deviation %	45.64	64.79	70.58	64.04	6.42
±20% index	28.67	15.38	0.00	4.20	99.65

Table 6 Deviations associated with different correlations (forced convection square-edged inlet, 130 data points)

Deviation range	Eq. (2)	Eq. (3)	Eq. (5)	Eq. (6)	Eq. (7)
Number of points below ±5%	44.00	4.00	7.00	2.00	46.00
Number of points between ±5–10%	74.00	20.00	17.00	9.00	32.00
Number of points between ±10–20%	8.00	77.00	60.00	60.00	40.00
Number of points between ±20–30%	4.00	23.00	23.00	29.00	12.00
Number of points above ±30%	0.00	6.00	23.00	30.00	0.00
Absolute maximum deviation %	26.45	49.44	68.54	41.24	24.31
Absolute minimum deviation %	0.05	2.90	0.28	0.98	0.05
Absolute average deviation %	6.52	15.72	20.76	21.17	9.02
±20% index	96.92	77.69	64.62	54.62	90.77

Table 7 Deviations associated with different correlations (mixed convection bell-mouth inlet, 365 data points)

Deviation range	Eq. (2)	Eq. (3)	Eq. (5)	Eq. (6)	Eq. (7)
Number of points below ±5%	8.00	0.00	20.00	0.00	55.00
Number of points between ±5–10%	4.00	0.00	20.00	0.00	208.00
Number of points between ±10–20%	3.00	0.00	35.00	0.00	98.00
Number of points between ±20–30%	6.00	0.00	38.00	0.00	4.00
Number of points above ±30%	344.00	365.00	252.00	365.00	0.00
Absolute maximum deviation %	263.33	344.90	334.40	334.64	22.03
Absolute minimum deviation %	1.12	38.99	0.51	49.32	0.17
Absolute average deviation %	128.46	185.44	103.66	200.72	8.66
±20% index	4.11	0.00	20.55	0.00	98.90

Table 8 Deviations associated with different correlations (forced convection bell-mouth inlet, 68 data points)

Deviation range	Eq. (2)	Eq. (3)	Eq. (5)	Eq. (6)	Eq. (7)
Number of points below ±5%	59.00	16.00	4.00	4.00	39.00
Number of points between ±5–10%	9.00	24.00	23.00	23.00	21.00
Number of points between ±10–20%	0.00	19.00	41.00	41.00	8.00
Number of points between ±20–30%	0.00	8.00	0.00	0.00	0.00
Number of points between ±30%	0.00	1.00	0.00	0.00	0.00
Absolute maximum deviation %	6.65	46.64	16.48	16.49	18.76
Absolute minimum deviation %	0.25	0.27	4.54	4.54	0.27
Absolute average deviation %	2.48	10.17	10.72	10.74	4.99
±20% index	100.00	86.76	100.00	100.00	100.00

than 20% deviation. These comparison results are also shown in Figures 18 to 20. As detailed in Tables 3 to 8, Eq. (7)—unlike the correlations of Gnielinski and Churchill—provides a very stable performance in all flow regions and predicts none of the experimental data for the three inlets with a deviation larger than 30%.

Based on the above observations, Gnielinski's and Churchill's correlations fail to give accurate predictions in the mixed convection region. This is directly due to the effect of free convection superimposed on the main flow, something Gnielinski and Churchill did not address in their works. As a matter of fact, in all convective flows, pure forced or free convection should be considered as extreme cases, and mixed convection should be considered as the general rule and not be overlooked. Because Eq. (7) is correlated with an extra independent variable (Grashof number) and accounts for the influence of different inlet configurations on the start and end of the transition region through different sets of constants for each inlet configuration, the correlation is much more accurate in the developing and fully developed mixed convection transition region in comparison to the other correlations available in the literature thus, it is recommended for this region. For the forced convection transition region, if the 20% deviation criterion is used, Eqs. (2) and (7) both give very good predictions of the experimental data for all three inlets, and they are recommended.

In a recent work, Ghajar et al. [16] used an artificial neural network (ANN) to predict the same set of experimental Nusselt numbers used above [1]. Using a three-layer, feed-forward neural network with eleven hidden neurons and the Levenberg-Marquardt back propagation method, they developed the following ANN heat transfer correlation:

$$\mathrm{Nu} = \mathrm{u}^3\{(\mathrm{u}^2)^2\mathrm{f}(\mathrm{u}^1\Phi + \mathrm{v}^1) + \mathrm{v}^2\} + \mathrm{v}^3 \tag{10}$$

where

$$\mathrm{f(s)} = [1 - exp(s)]^{-1}$$

$$\Phi = \begin{bmatrix} \mathrm{Re}_{\mathrm{normal}} \\ \mathrm{Pr}_{\mathrm{normal}} \\ \mathrm{Gr}_{\mathrm{normal}} \\ \mathrm{x/D}_{\mathrm{normal}} \\ \left(\dfrac{\mu_b}{\mu_w}\right)^{0.14}_{\mathrm{normal}} \end{bmatrix} = \begin{bmatrix} 2(\mathrm{Re} - \mathrm{Re}_{\min})/(\mathrm{Re}_{\max} - \mathrm{Re}_{\min}) - 1 \\ 2(\mathrm{Pr} - \mathrm{Pr}_{\min})/(\mathrm{Pr}_{\max} - \mathrm{Pr}_{\min}) - 1 \\ 2(\mathrm{Gr} - \mathrm{Gr}_{\min})/(\mathrm{Gr}_{\max} - \mathrm{Gr}_{\min}) - 1 \\ 2(\mathrm{x/D} - \mathrm{x/D}_{\min})/(\mathrm{x/D}_{\max} - \mathrm{x/D}_{\min}) - 1 \\ 2\left(\left(\dfrac{\mu_b}{\mu_w}\right)^{0.14} - \left(\dfrac{\mu_b}{\mu_w}\right)^{0.14}_{\min}\right) \Big/ \left(\left(\dfrac{\mu_b}{\mu_w}\right)^{0.14}_{\max} - \left(\dfrac{\mu_b}{\mu_w}\right)^{0.14}_{\min}\right) - 1 \end{bmatrix}$$

The entries of the vector Φ represent the normalized Reynolds number, Prandtl number, Grashof number, x/D, and μ ratio, respectively. In their study, only 80% of the experimental data (denoted by M_a in Figure 21) for each inlet were used to establish the correlation's constant matrices, as indicated in Eq. (10). The rest of the data (i.e., 20%, as denoted by M_b in Figure 21) were used for the network testing. The numerical values for the matrices and scalars for different inlet configurations are given in [16]. The comparison between the predicted and experimental Nusselt numbers is shown in Figure 21. It can be seen that the accuracy of the correlation is superb, and the majority of the experimental data were predicted with less than 5% deviation. However, as discussed in Ghajar et al. [16], unlike the semi-empirical equations, the physical meanings are difficult to be extracted from the ANN correlations, and research on extracting knowledge from this type of correlation should be undertaken. Because the ANN correlations, are very accurate, Eq. (10) is also recommended to be used in the transition region.

FLOW REGIME MAP

Ghajar and Tam [3] developed a flow regime map for determining the boundary between forced and mixed convection in a plain horizontal tube with re-entrant, square-edged, and bell-mouth inlets under a uniform wall heat flux boundary condition. As discussed earlier, heating a fluid flowing in a horizontal tube produces secondary flow. The fluid near the tube wall, due to its higher temperature and lower density, circulates upward, while the fluid near the central region of the tube, having a lower temperature and a higher density, circulates downward. These counter-rotating, transverse vortices that are superimposed on the streamwise main flow due to free convection (buoyancy influences) can significantly increase the forced convection heat transfer. It is important to realize that heat transfer in combined forced and free (or mixed) convection can be significantly different from its values in both pure free and pure forced convection. Actually, buoyancy forces (free convection effects) are present in any forced convection flow, and for design purposes, it is of interest to know when they can be neglected and when they have to be accounted for. Such an investigation is made difficult by the large number of influencing parameters. Buoyancy influences forced convection heat transfer in horizontal tubes in ways that depend on Reynolds, Prandtl, and Grashof numbers as well as the tube inlet configuration, wall boundary condition, and the length-to-inside diameter ratio of the tube [1]. This makes it difficult and sometimes even dangerous to make a

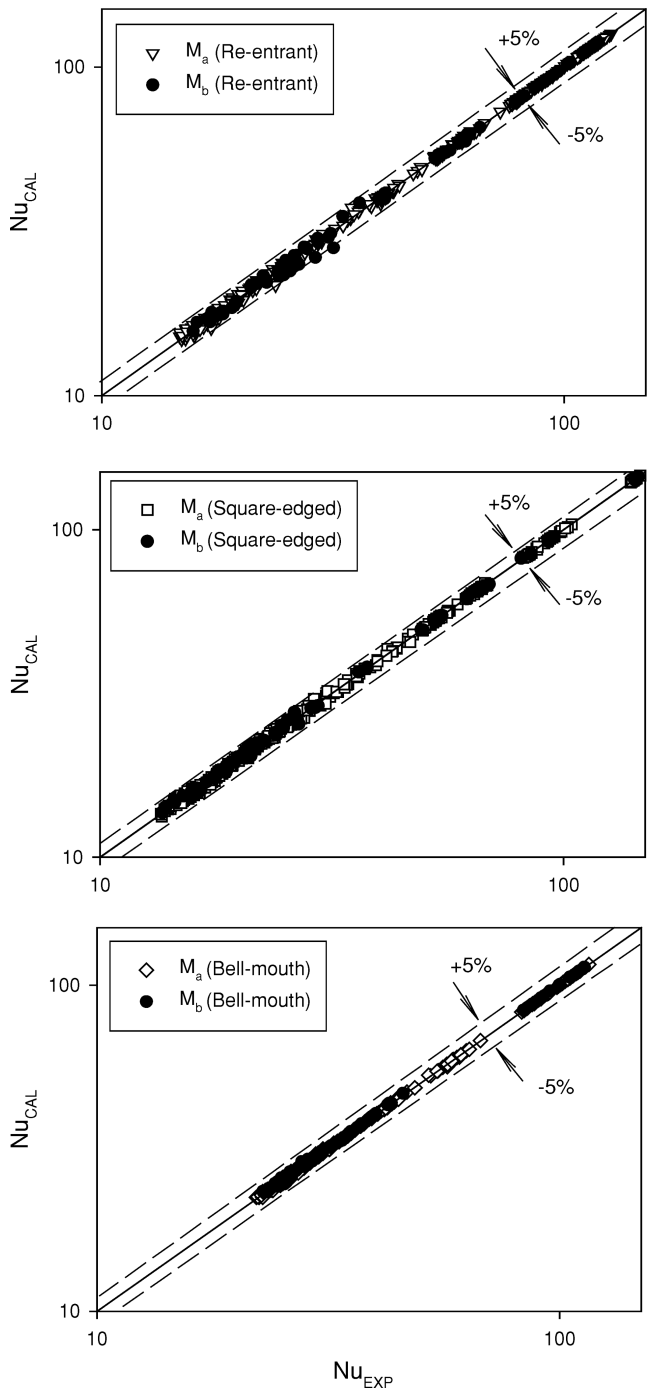

Figure 21 Comparisons between experimental Nusselt numbers and those predicted by Eq. (10), the ANN-based transition region heat transfer correlation.

priori assumptions concerning buoyancy effects in internal flow. Ghajar and Tam [3] used their extensive mixed and forced convection experimental heat transfer data in all flow regimes for three inlet configurations [1, 2] and their heat transfer correlations (see Eqs. [7–9]) to develop the flow regime map shown in Figure 22. Their flow regime map is applicable to all flow regimes (laminar, transition, turbulent) and the three inlets (re-entrant, square-edged, bell-mouth). From the flow regime map,

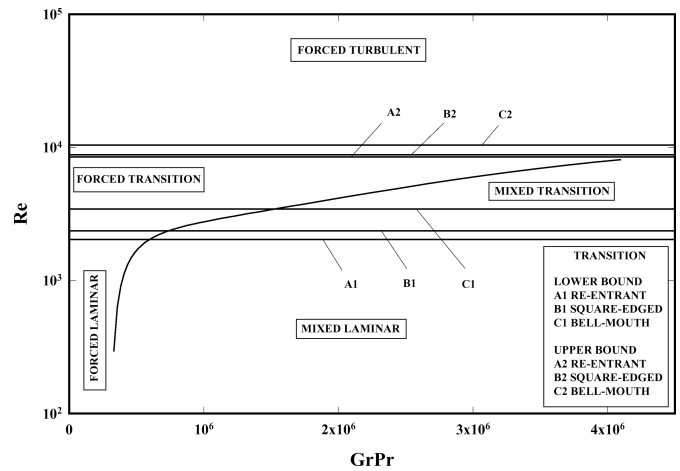

Figure 22 Flow regime map for flow in horizontal tubes with three different inlet configurations and uniform wall heat flux.

for any forced flow represented by a given Reynolds number, the value of the parameter GrPr at a particular x/D location indicates whether it is necessary to consider buoyancy effects. For the identified pure forced or mixed convection region heat transfer regime, the heat transfer correlations presented in this paper, Eqs. (7–9), are recommended for heat transfer calculations.

CONCLUDING REMARKS

A detailed discussion of the behavior of heat transfer in the transition region for a horizontal tube under uniform wall heat flux boundary condition was provided in this study, and the role of mixed convection and the inlet configuration on the start and end of the heat transfer transition region were clearly established. Several heat transfer correlations for the transition region available in the open literature were reviewed. The applicability of each correlation in the transition region based on a comparison with an extensive set of experimental data was established. It was concluded that Eqs. (2) and (7) give an excellent all-around performance in the forced convection transition flow. In the mixed convection transition flow, only Eq. (7) gives excellent performance. Finally, for the determination of the boundary between forced and mixed convection in a horizontal tube with uniform wall heat flux and different inlet configurations, a flow regime map was presented. The flow regime map can be used to assist the heat exchanger designer in determining the influence of buoyancy in a horizontal tube with uniform wall heat flux for a specified inlet configuration in all flow regimes. For the identified pure forced or mixed convection heat transfer regime, heat transfer calculations can be made based on the recommended correlations.

NOMENCLATURE

a,b,c constants in Eq. (7)
c_p specific heat at constant pressure, J/kg K

D	tube inside diameter, m
f	friction factor
g	acceleration due to gravity, m^2/s
Gr	Grashof number ($= g\beta\rho^2 D^3(T_w - T_b)/\mu^2$)
h	convective heat transfer coefficient, W/m^2 K
h_b	convective heat transfer coefficient being measured at the bottom of the tube, W/m^2 K
h_t	convective heat transfer coefficient being measured at the top of the tube, W/m^2 K
j	Colburn j-factor ($= St\ Pr^{0.67}$)
k	thermal conductivity, W/mK
$\dot{m}$	mass flow rate, kg/m^2 s
M_a	number of experimental points used for training the neural network
M_b	number of experimental data points used for testing the neural network
Nu	Nusselt number ($= hD/k$)
p	exponent in asymtotic solution
Pr	Prandtl number ($= \mu c_p/k$)
Re	Reynolds number ($= 4\dot{m}/\pi D\mu$)
St	Stanton number ($=$ Nu/Re Pr)
T	temperature, K
u	constant matrix in Eq. (10)
v	constant matrix in Eq. (10)
x	distance from entrance, m

Greek Symbols

β	coefficient of thermal expansion, K^{-1}
μ	absolute or dynamic viscosity, Ns/m^2
ρ	density, kg/m^3
Φ	normalized input vector

Subscripts

b	evaluated at bulk temperature
CAL	calculated
EXP	experimental
l	laminar
lc	laminar flow at critical Reynolds number
t	turbulent
trans	transition
w	wall

REFERENCES

[1] Ghajar, A. J., and Tam, L. M., Heat Transfer Measurements and Correlations in the Transition Region for a Circular Tube with Three Different Inlet Configurations, *Experimental Thermal and Fluid Science*, vol. 8, pp. 79–90, 1994.

[2] Ghajar, A. J., and Tam, L. M., Flow Regime Map for a Horizontal Pipe with Uniform Wall Heat Flux and Three Inlet Configurations, *Experimental Thermal and Fluid Science*, vol. 10, pp. 287–297, 1995.

[3] Tam, L. M., and Ghajar, A. J., The Unusual Behavior of Local Heat Transfer Coefficient in a Circular Tube with a Bell-Mouth Inlet, *Experimental Thermal and Fluid Science*, vol. 16, pp. 187–194, 1998.

[4] Sieder, E. N., and Tate, G. E., Heat Transfer and Pressure Drop in Liquids in Tubes, *Ind. Eng. Chem.*, vol. 28, pp. 1429–1435, 1936.

[5] Hausen, H., New Equations for Heat Transfer in Free or Force Flow, *Allg. Warmetchn.*, vol. 9, no. 4/5, pp. 75–79, 1959.

[6] Hufschmidt, W., Burck, E., and Riebold, W., Determination of Local and Average Heat Transfer Coefficients in Tubes at High Heat Fluxes, *Int. J. Heat Mass Transfer*, vol. 9, no. 6, pp. 539–565, 1966.

[7] Reinicke, H., Uber den Warmeubergang von kurzen durchstromten Rohren und querumstromten Zylindern verschiedener Anordnung an zahe Flussigkeiten verschiedener Prandtl-Zahl bei kleinen Temperaturdifferenzen (Heat Transfer for Viscous Liquids of Different Prandtl Number in Flow Through Tubes and Across Cylinders of Different Orientation for Small Temperature Differences), Dissertation D 17, Techn. Hochschule Darmstadt, Germany, 1969.

[8] Schlunder, E. U., Uber eine zusammenfassende Darstellung der Grundgesetze des konvektiven Warmeuber-gangs (An Overall Representation of the Basic Laws of Convective Heat Transfer), *Verfahrenstechnik*, vol. 4, no. 1, pp. 11–16, 1970.

[9] Kakac, S., Shah, R. K., and Aung, W., *Handbook of Single-phase Convective Heat Transfer*, Wiley, New York, 1987.

[10] Gnielinski, V., New Equations for Heat and Mass Transfer in Turbulent Pipe and Channel Flow, *Int. Chem. Eng.*, vol. 16, pp. 359–368, 1976.

[11] Churchill, S. W., Comprehensive Correlating Equations for Heat, Mass and Momentum Transfer in Fully Developed Flow in Tubes, *Ind. Eng. Chem. Fundam.*, vol. 16, no. 1, pp. 109–116, 1977.

[12] Shah, R. K., and Johnson, R. S., Correlations for Fully Developed Turbulent Flow Through Circular and Noncircular Channels, *Sixth Nat. Heat and Mass Transfer Conf.*, Indian Inst. Technology, Madras, India, pp. D-75–D-95, 1981.

[13] Pettukhov, B. S., and Kirillov, V. V., The Problem of Heat Exchange in the Turbulent Flow of Liquids in Tubes, *Teploenergetika*, vol. 4, no. 4, pp. 63–68, 1958 (in Russian).

[14] Prandtl, L., *Fuhrer durch die Stromungslehre, Vieweg, Braunschweig*, p. 359, 1944; English Translation, Blackie, London, 1952.

[15] Churchill, S. W., and Usagi, R., A General Expression for the Correlation of Rates of Transfer and Other Phenomena, *AICHE*, vol. 18, no. 6, pp. 1121–1128, 1972.

[16] Ghajar, A. J., Tam, L. M., and Tam, S. C., Improved Heat Transfer Correlation in the Transition Region for a Circular Tube with Three Inlet Configurations Using Artificial Neural Network, *Heat Transfer Engineering*, vol. 25, no. 2, pp. 30–40, 2004.

Lap Mou Tam received his Ph.D. in 1995 from Oklahoma State University, the School of Mechanical and Aerospace Engineering, Stillwater, Oklahoma. In 1996, he joined the University of Macau as an assistant professor and is now an associate professor and department head of electromechanical engineering at the University of Macau, Macau, China. In 2001, he was appointed by the University of Macau to serve as the chairman of board of directors in the Institute for the Development and Quality, a non-profit institute

providing mechanical- and electromechanical-related engineering services to the public. His research interests include single and multiphase heat transfer, chaos, fire engineering, and indoor air quality. He is a senior member of the Chinese Mechanical Engineering Society.

Afshin J. Ghajar is a Regents professor and director of graduate studies in the School of Mechanical and Aerospace Engineering at Oklahoma State University. He received his B.S., M.S., and Ph.D. all in mechanical engineering from Oklahoma State University. His expertise is in experimental and computational heat transfer and fluid mechanics. Dr. Ghajar has been a summer research fellow at Wright Patterson AFB (Dayton, Ohio) and Dow Chemical Company (Freeport, Texas). He and his coworkers have published over 100 reviewed research papers. He has received several outstanding teaching/service awards: the Regents Distinguished Teaching Award, the Halliburton Excellent Teaching Award (twice), the Mechanical Engineering Outstanding Faculty Award for Excellence in Teaching and Research (twice), and the Golden Torch Faculty Award for Outstanding Scholarship, Leadership, and Service by the Oklahoma State University/National Mortar Board Honor Society. Dr. Ghajar is a fellow of the American Society of Mechanical Engineers (ASME) and the Editor-in-Chief of *Heat Transfer Engineering*.